Journal of Theoretical and Applied Physics (2020) 14:339–348
https://doi.org/10.1007/s40094-020-00390-5

RESEARCH

Fabrication of Au/ZnO/MWCNTs electrode and its characterization for electrochemical cholesterol biosensor

Davood Ghanei Agh Kaariz[1] · Elham Darabi[1] · Seyed Mohammad Elahi[1]

Received: 16 July 2020 / Accepted: 9 August 2020 / Published online: 19 August 2020

Abstract

In this work, a new sensitive enzyme-based electrode for electrochemical cholesterol biosensor was fabricated based on a nanocomposite of Au nanoparticles, ZnO nanoparticles and multi-wall carbon nanotubes (Au/ZnO/MWCNTs). The nanocomposite was prepared by sol–gel method and deposited on FTO substrate by dip coating, followed by cholesterol oxidase (ChOx) enzyme immobilized (ChOx/Au/ZnO/MWCNTs). Structural properties and morphology of the nanocomposite have been studied using X-ray diffraction (XRD) and Field emission scanning electron microscopy (FESEM). The sample was subjected to Fourier transform infrared spectroscopy (FTIR) to determine functional groups. Electrochemical behavior of the electrode was studied by cyclic voltammetry (CV) and differential pulse voltammetry (DPV) techniques as a function of cholesterol concentration. Electrochemical impedance spectroscopy (EIS) was also considered to study of surface modified electrodes. The ChOx/Au/ZnO/MWCNTs electrode has been found to have enhanced electron transfer and display excellent analytical linear performances. The fabricated electrode exhibited low detection limit (0.1 µM), high sensitivity (25.89 µA/µM) evaluated from DPV data in the detection range of 0.1–100 µM and high selectivity in the determination of cholesterol over glucose and uric acid. The application of the ChOx/Au/ZnO/MWCNTs electrode in detection of cholesterol in human serum was also confirmed.

Keywords Electrochemical biosensor · Cholesterol · Cholesterol oxidase · Au nanoparticles · ZnO nanoparticles · Multi-wall carbon nanotubes · Au/ZnO/MWCNTs nanocomposite

Introduction

Cholesterol ($C_{27}H_{46}O$) is one of the most important biomolecules and is one of the essential components of body. Its major role is to provide strength and flexibility to the biological membrane of cells and is present in several nerve tissues, brain and also serves as a source for preparation of fatty acids. Despite the undeniable importance of cholesterol, the excessive amounts of it can be dangerous for human health. The maximum amount of cholesterol in healthy human serum should not be more than 200 mg/dL (5.17 mM) [1]. The presence of excess cholesterol in the blood serum causes arteriosclerosis, which can lead to heart disease, arterial obstruction, kidney disease, and myocardial infarction. On the other hand, low levels of cholesterol in the blood can lead to anemia. Therefore, cholesterol level in the blood serum is one of the important parameters that should always be under control. Today, there is a great interest to find an exact, simple and user friendly method to determine cholesterol level. So far, many methods such as classical chemical methods, enzymatic assays, chromatography, mass spectrometry, colorimetry and electrochemical methods have been used to determine cholesterol level [2–4]. Recent advances in cholesterol biosensors involve introducing nanomaterials to achieve better performance and low-cost biosensor in comparison with the traditional methods [5–7]. On the other hand, enzyme-based electrochemical biosensors have been widely considered in order to determine cholesterol due to their low cost, rapid determination and high selectivity [8–10]. Cholesterol oxidase (ChOx) is the most commonly used analytes to provide an enzyme-based cholesterol biosensor [11]. An enzymatic reaction using ChOx is as follows in which ChOx accelerates the oxidation of cholesterol to H_2O_2 and Cholest-4-en-3-one [11].

✉ Elham Darabi
e.darabi@srbiau.ac.ir

[1] Department of Physics, Faculty of Sciences, Science and Research Branch, Islamic Azad University, Tehran, Iran

$$\text{Cholesterol} + O_2 \xrightarrow{\text{ChOx}} \text{Cholest} - 4 - \text{en} - 3 - \text{one} + H_2O \quad (1)$$

Biocompatible nanomaterials open a promising field toward the development of enzyme-based electrochemical biosensors. Sensors based on carbon nanotubes (CNTs) have shown excellent performance in determining biomolecules such as cholesterol, glucose, protein cancer biomarkers and many others [7, 8, 12–14]. Owing to their good conducting property, chemical stability and high surface area, CNTs can be used for low level detection of biomolecules. CNTs enhance the electrode surface coverage and can be used as the interface between electrodes and the oxidation–reduction center in biomolecules. The ChOx on the CNTs-based electrode showed a pair of semi-Gaussian peak of oxidation–reduction for the direct transmission of electrons [9, 11].

Studies also showed that modification of CNT-based electrodes with metal and metal oxide nanoparticles exhibited a huge capacitive-current in some electrolytes. The main roles of nanomaterials are to provide a higher surface area for the immobilization of biomolecules and amplification of signals. So, they can lower the working potential and enhances the selectivity and sensitivity of the biosensor [15–18]. The use of metal nanoparticles such as Au, Ag or Pt in electrochemical biosensors has become very popular, due to their excellent biocompatibility, unique role in charge transfer for the improvement of conductivity, catalytic activity and their ability to provide a stable immobilization for biomolecules [6, 17]. Shahid Mehmood et al. studied the effect of different concentrations of Au nanoparticles in the electrochemical response of modified Au-MWCNT electrodes in determining cholesterol [17]. The charge transfer rate is dependent on the concentration of the Au nanoparticles, which has an upward trend with the increase in concentration. Various metal oxide nanomaterials have received great attention for biosensing because of characteristics such as biocompatibility, catalytic and optical properties and electron transfer kinetics. Among them, zinc Oxide (ZnO) as a wide direct band gap semiconductor (3.37 eV) exhibits a very efficient electron transfer. In addition, ZnO nanocatalysts have an isoelectric point (IEP) above 9.5, which is useful for stabilizing low biomaterials such as cholesterol oxidase (IEP ~ 5.0) in buffer solutions [19]. Furthermore, the biocompatible nature of ZnO nanoparticles makes it a good candidate to interact with biomolecules at different temperature and pH levels [20].

Although modified CNTs-based biosensors are promising, much further advancement is needed to be addressed until they can be used as a rapid, accurate and cost-effective clinical tool. The creation of nanohybrid materials can be regarded as an efficient strategy for developing high-performance devices and even new detection techniques such as photoelectrochemical biosensing [21, 22]. So, the major aim of the present work is to develop a simple and sensitive modified electrode for the efficient determination of cholesterol and a promising candidate for photoelectrochemical biosensing.

In this paper, Au/ZnO/MWCNTs nanocomposite was prepared by sol–gel method and deposited on Ar plasma treated FTO glass substrate by dip coating. Then the enzyme of cholesterol oxidase was stabilized on the electrode. To examine the effect of Au on the sensor properties, ZnO/MWCNTs electrode was also fabricated and the electrochemical performance of two electrodes in determination of cholesterol was studied by electrochemical measurements. The synthesized nanocomposites were also characterized with X-ray diffraction (XRD), Field emission scanning electron microscopy (FESEM) and Fourier transform infrared spectroscopy (FTIR).

Materials and methods

Materials

FTO coated glass with a resistance of 40 O/sq was used as conductive substrates. Multi-wall Carbon nanotubes over 1.0 micron in length with the outer diameter of about 30 nm were obtained from US nano-Company. Nitric acid, zinc acetate dihydrate ($Zinc(Acc)_2.2H_2O$) and Tetra chloric acid ($HAuCl_4$) were purchased from Merck Company. Sodium hydroxide (NaOH) and other chemical materials, such as cholesterol, NaH_2PO_4, Triton X-100, ethanol and ChOx enzyme have been provided from the Sigma Aldrich Company. Phosphate buffer solution (PBS, 0.1 M, pH = 7) was prepared with different NaH_2PO_4 ratios.

Synthesis of ZnO/MWCNTs and Au/ZnO/MWCNTs nanocomposites

Functionalization of CNTs is the first step in the preparation of nanocomposites and plays an important role in facilitating the bonding and placement or loading of particles on the surface wall of the MWCNTs. It increases the internal energy of the MWCNTs and generates active sites on the surface of the MWCNTs. In this study, certain amount of MWCNTs was treated with 80 mL of aqueous nitric acid. Mixture of MWCNTs and acid solution were heated until all the acid was evaporated. After that, the functionalized MWCNTs were washed thoroughly with distilled water until the neutral pH value was obtained. Sample was then dried at 140° C for 2 h.

To prepare ZnO/MWCNTs nanocomposite, 2.2 gr zinc acetate and 4 gr sodium hydroxide was dissolved into a solution of 35 mL distilled water and 40 mL ethanol. The ultimate solution was stirred for 1 h. After that, 47 mg of

functionalized carbon nanotubes was added to the above mixture and dispersed using ultrasound bath for 1 h. Then, the mixture was maintained at 120 °C for 12 h. To prepare nanopowder, the precipitate was collected by centrifugation, washed several times by distilled water and annealed at 250 °C for 30 min.

For preparation Au/ZnO/MWCNTs nanocomposites, the 0.1 molar solution of $HAuCl_4$ in distilled water was added drop wise into the mixture of zinc acetate and sodium hydroxide while stirring before adding carbon nanotubes. Then the same process was repeated to obtain Au/ZnO/MWCNTs nanocomposites.

Fabrication ZnO/MWCNTs/FTO and Au/ZnO/MWCNTs/FTO electrodes

The ZnO/MWCNTs/FTO and Au/ZnO/MWCNTs/FTO electrodes were fabricated by deep coating method. The 2×2 cm^2 FTO glass substrates were firstly washed with alcohol and acetone several times in ultrasonic bath then were modified by Ar plasma treatment for 10 min. For each electrode fabrication, the modified FTO substrate was immersed in its ultimate solution for 12 h and after taking out, it was annealed at 250 °C for 30 min.

Stabilizing the ChOx enzyme on the electrodes

In order to stabilize the enzyme on the electrodes, 1 mg of the enzyme was dissolved in distilled water and physically dispersed on the surface of the electrodes. Then, the electrodes were stored in refrigerator at a temperature of 4° C until it was analyzed (usually up to about 3 days).

Characterization techniques

The crystalline structure of nanocomposites was characterized using X-ray diffraction (XRD, D8 model, 2002, Bruker Company) operating with Cu Kα radiation (λ = 0.154060 nm). Field emission scanning electron microscopy (FESEM, JEOL JEM6700F) was used to investigate the morphology. A Fourier transform infrared spectroscopy (FTIR, Perkin-Elmer) was employed to demonstrate the chemical bonds and surface chemistry of the prepared samples in the range of 400–4000 cm^{-1}. Electrochemical measurements were performed with a three-electrode potentiostat/galvanostat (Emstae 3T). Standard Platinum wire counter electrode and Ag/AgCl reference electrode used to setup the electrochemical cell. ZnO/MWCNTs, ChOx/ZnO/MWCNTs, Au/ZnO/MWCNTs and ChOx/Au/ZnO/MWCNTs were used as working electrode. All the tests were carried out at the ambient temperature of laboratory and the supporting electrolyte was the 0.1 molar phosphate buffer solution (PBS) at a pH of 7.0. Voltammetric measurements (CV and DPV) were performed to determine cholesterol in the potential range of 0–1 V. Cyclic voltammetry (CV) was recorded in the 30 mL PBS at the scan rate of 100 mV/s. Differential pulse voltammetry (DPV) was done at the pulse amplitude of 25 mV and the scan rate of 100 mV/s in the 30 mL PBS and 1 mL NaCl (0.1 molar) as supporting electrolyte. Electrochemical impedance spectroscopy (EIS) was used to investigate the surface of electrodes and its data is presented in the form of Nyquist plot. The impedance was measured in the frequency range from 10^5 to10^{-1} Hz in a potential of open-circuit value of +0.25 V versus Ag/AgCl with a sinusoidal signal of 10 mV in the presence of 4 mM $[Fe(CN)_6]^{3-/4-}$ mixture (1:1).

Results and discussion

Figure 1 shows the XRD spectrum for ZnO/MWCNTs and Au/ZnO/MWCNTs nanocomposites. It is observed that the XRD pattern of Au/ZnO/MWCNTs is very similar to that of ZnO/MWCNTs, indicating the formation of Au in addition of ZnO crystalline structure. The crystalline structure parameters of the nanocomposites are summarized in Table 1. For ZnO/MWCNTs nanocomposite, the diffraction peaks at 2θ = 31.75°, 34.40°, 36.19°, 56.53°, 62.81°, and 67.89°, respectively, corresponds to (100), (002), (101), (110), (103) and (112) planes which can be indexed to hexagonal wurtzite structure of ZnO (JCPDS Card No.01-080-0074).The diffraction peaks at 25.81 °, 47.56 ° and 53.54 ° corresponds to the carbon of the MWCNTs and reveals the crystallinity of the MWCNTs (JCPDS Card No.00-026-1076). The XRD pattern of Au/ZnO/MWCNTs nanocomposite also presents diffraction peaks related to ZnO and MWCNTs crystalline structure.

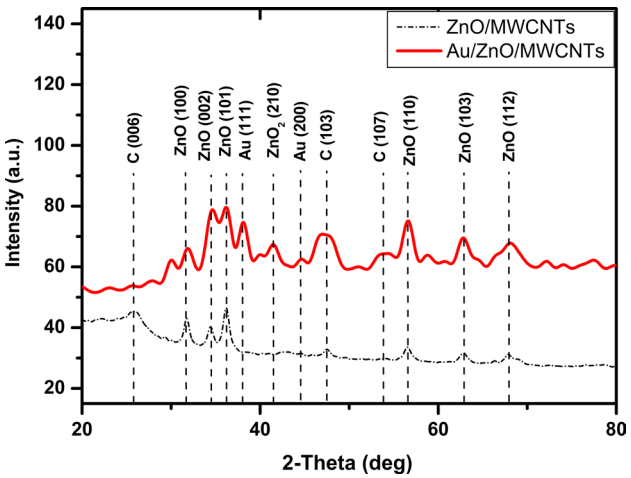

Fig. 1 XRD patterns of ZnO/MWCNTs and Au/ZnO/MWCNTs nanocomposites

Table 1 The XRD data for ZnO/MWCNTs and Au/ZnO/MWCNTs nanocomposites

Nanocomposite	Peak position (2Θ) (Degree)	Material	hkl	Rel. Int (%)	Crystallite size(nm)
ZnO/MWCNTs	25.81	C	006	44.36	27.2
	47.56	C	103	39.66	23.3
	53.54	C	107	29.78	31.7
	31.75	ZnO	100	59.66	13.1
	34.40	ZnO	002	47.32	13.2
	36.19	ZnO	101	100.00	13.3
	56.53	ZnO	110	16.80	14.3
	62.81	ZnO	103	29.82	14.8
	67.89	ZnO	112	21.80	15.2
Au/ZnO/MWCNTs	25.62	C	006	31.6	30.61
	47.56	C	103	39.66	23.3
	53.54	C	107	29.78	31.7
	31.83	ZnO	100	51.64	26.2
	34.51	ZnO	002	74.4	17.6
	36.23	ZnO	101	100	35.4
	56.57	ZnO	110	42.84	19.1
	62.82	ZnO	103	28.99	16.2
	67.88	ZnO	112	33.57	47.88
	41.38	ZnO_2	210	31.01	18.0
	38.00	Au	111	75.14	30.5
	44.60	Au	200	31.16	26.7

In addition, two peaks at 38 ° and 44.6 ° is observed, which can be ascribed to the (111) and (200) planes of face-centered cubic Au (JCPDS Card No.00-001-1172). In this spectrum, there is another peak at 41.3 ° corresponds to ZnO_2crystalline structure (JCPDS Card No.01-080-0074). The grain size of crystallites, listed in Table 1, is estimated using well-known Scherer formula [23].

The morphology of functionalized MWCNTs (*f*-MWCNTs), ZnO/MWCNTs and Au/ZnO/MWCNTs nanocomposites which was observed by FESEM is presented in Fig. 2a–c. Figure 2a shows a well-dispersed carbon nanotubes network, although functionalized MWCNTs are and twisted together. The FESEM image shown in Fig. 2b confirms the formation of ZnO nanoparticles on carbon nanotubes with a symmetric distribution of spherical

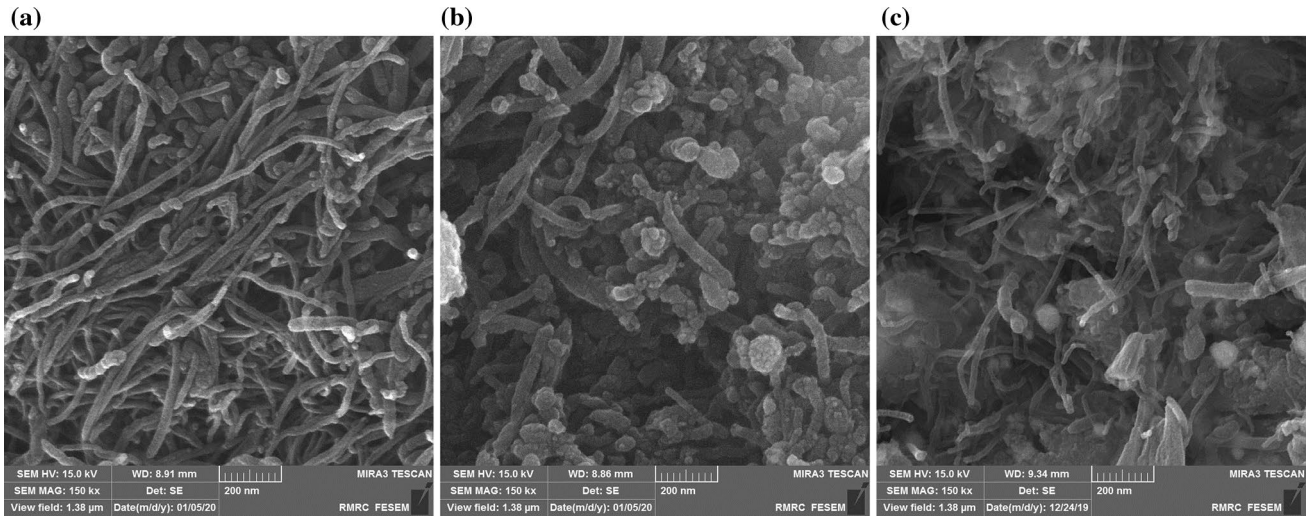

Fig. 2 FESEM images of **a** *f*-MWCNTs, **b** ZnO/MWCNTs nanocomposite and **c** Au/ZnO/MWCNTs nanocomposite

nanoparticles. It seems ZnO nanoparticles are well-placed on the MWCNTs wall which is important for tight bonding of the nanocomposite to the electrode surface, cholesterol oxidase enzyme immobilization and increase in charge transfer rate. These observations are also well-visible for the Au/ZnO/MWCNTs nanocomposite in Fig. 2c. It is also seen that Au particles which have almost spherical shapes are randomly distributed on the surface of the nanotubes.

The FTIR spectra of *f*-MWCNTs, ZnO/MWCNTs and Au/ZnO/MWCNTs nanocomposites are shown in Fig. 3. The characteristic peak around3470 cm^{-1} corresponds to the stretching vibration of OH bond, related to the water molecule bound on the surface of the nanotubes. The band around 1430 cm^{-1} is associated with the vibration of the carbon skeleton of the carbon nanotubes [24]. The band at 1021 cm^{-1} indicates the existence of a strong C–O stretching mode. The FTIR spectrum of the ZnO/MWCNTs and Au/ZnO/MWCNTs nanocomposites reveals some differences. The band around 3470 cm^{-1} is missed in ZnO/MWCNTs and Au/ZnO/MWCNTs nanocomposites spectra, due to the temperature dependent behavior of OH stretching modes [25] and the effect of annealing during nanopowder synthesis. It can be observed that band around 1021 cm^{-1} is much lower in the nanocomposites than that of functionalized MWCNTs, suggesting that the surface of MWCNTs has been covered by nanoparticles. The FTIR spectrum of the two nanocomposites also exhibits a band at 440 cm^{-1} arising due to Zn–O vibration [26].

Two electrodes were prepared using the synthesized Au/ZnO/MWCNTs nanocomposite as described in Sect. 2.3, which one of them modified by ChOx enzyme. Two electrodes were also prepared based on ZnO/MWCNTs nanocomposite with the same protocol for comparison purposes.

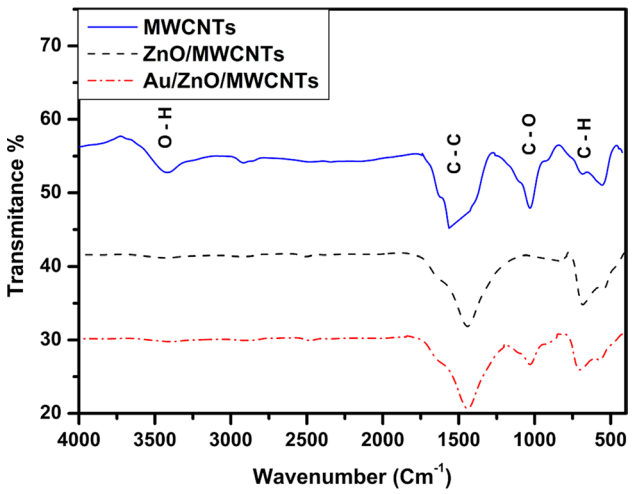

Fig. 3 FTIR spectra of *f*-MWCNTs, ZnO/MWCNTs and Au/ZnO/MWCNTs nanocomposites

Electrodes were electrochemically characterized in 0.1 M PBS (pH 7) by CV, DPV and EIS techniques.

Figure 4 shows cyclic voltammograms of (a) ZnO/MWCNTs, (b) Au/ZnO/MWCNTs, (c) ChOx/ZnO/MWCNTs and (d) ChOx/Au/ZnO/MWCNTs electrodes at various concentrations of cholesterol in supporting electrolyte (0.1, 0.3, 0.5, 1, 2, 3, 4, 5and 6 mM)at a scan rate of 100 mV/s. The cyclic voltammograms for all electrodes are reversible and show redox peaks. This means oxidation and reduction reactions are well-done. It is clearly seen that the rate of oxidation and reduction increases by increase in cholesterol concentration in the electrolyte for all electrodes. Comparing the voltammograms of ZnO/MWCNTs and Au/ZnO/MWCNTs electrodes at a constant cholesterol concentration shows an obvious increase in the anodic peak current and oxidation–reduction rate for Au/ZnO/MWCNTs electrode. This is due to the increase in the number of free electrons and enhanced charge transfer rate between electrolyte and electrode. The ChOx enzyme-based electrodes exhibit a higher current response to cholesterol, compared with non-enzymatic electrodes. This is due to the well-known reaction mechanism of cholesterol oxidation and the determination of H_2O_2 as described in Eq. (1) [11]. Since the H_2O_2 is the byproduct of cholesterol oxidation, the electroreduction current of H_2O_2 can be further detected by the ChOx enzyme-based electrodes.

The calibration graphs for all electrodes are shown in Fig. 5. It can be seen that the reduction current (I) varies linearly according to cholesterol concentration (C) in the entire concentration range for all electrodes. Typically, the linear equation for the calibration curve of Au/ZnO/MWCNTs electrode was found to be $y = 1.6539x + 11.062$ with correlation coefficient of $R^2 = 0.9933$.

Figure 6 displays Nyquist plots for all electrodes in the frequency range from 10^5 to 10^{-1} Hz in the presence of 4 mM $[Fe(CN)_6]^{3-/4-}$ mixture. As can be seen, all electrodes exhibit both a semicircle and a straight line. The diameter of the semicircle in a Nyquist plot represents the charge transfer resistance (R_{ct}), and the straight line shows the diffusion-related process. The smallest semicircle diameter is obtained for Au/ZnO/MWCNTs electrode, indicating improved conductivity and low R_{ct}. Obviously; it is due to the enhanced charge transfer at the surface of Au modified electrodes. However, an increase in the R_{ct} values is observed after ChOx immobilization onto the surface of ZnO/MWCNTs and Au/ZnO/MWCNTs electrodes. These changes are strong proof that ChOx could have been immobilized onto the surface of electrodes. Generally, the EIS results are in good agreement with those of cyclic voltammetry.

All electrodes were also studied by differential pulse voltammetry (DPV) to achieve more accurate and sensitive voltammetric responses. Differential pulse voltammograms are demonstrated in Fig. 7 over the cholesterol concentration

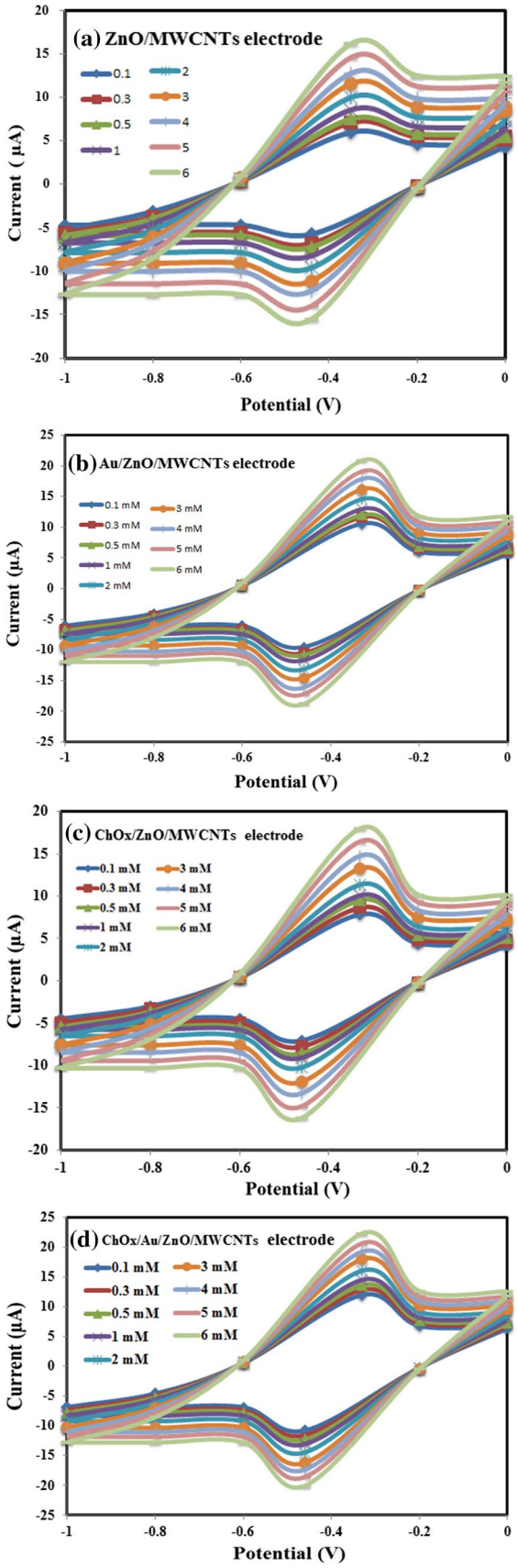

◂ **Fig. 4** Cyclic voltammograms of **a** ZnO/MWCNTs, **b** Au/ZnO/MWCNTs, **c** ChOx/ZnO/MWCNTs and **d** ChOx/Au/ZnO/MWCNTs electrodes, examined in 0.1 M PBS (pH 7.0) containing various concentrations of cholesterol (0.1, 0.3, 0.5, 1, 2, 3, 4, 5 and 6 mM) at a scan rate of 100 mVs^{-1}

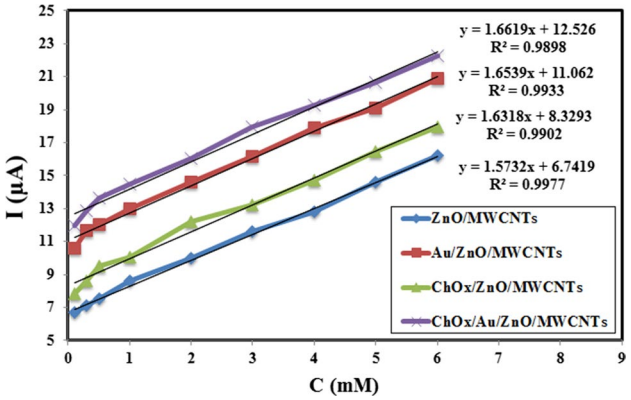

Fig. 5 Calibration graphs for ZnO/MWCNTs,Au/ZnO/MWCNTs,ChOx/ZnO/MWCNTs and ChOx/Au/ZnO/MWCNTs electrodes, obtained from CV data

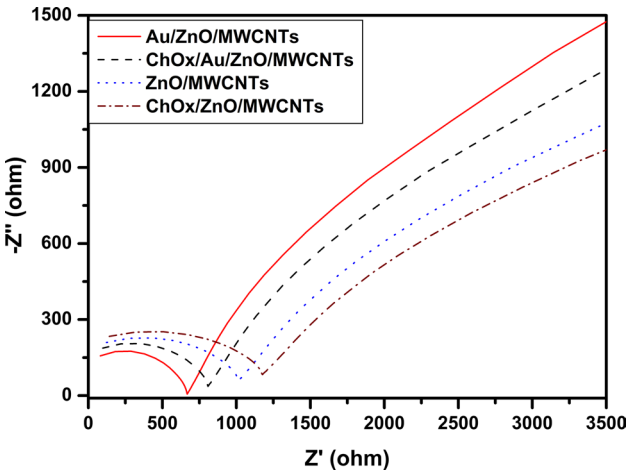

Fig. 6 Nyquist plots for all electrodes in the frequency range from 10^5 Hz to 10^{-1} Hz

range from 0.1 μM to 6 mM. It is clearly seen that during the addition of cholesterol to the electrolyte, there is an increase in anodic peak current for all electrodes. As expected, the highest current response to cholesterol is observed for ChOx/Au/ZnO/MWCNTs electrode due to the high immobilization and direct electron transfer between the active sites of immobilized ChOx and electrode. The obtained limit of detection (LOD) for this electrode was 0.1 μM in the detection range of 0.1–100 μM.

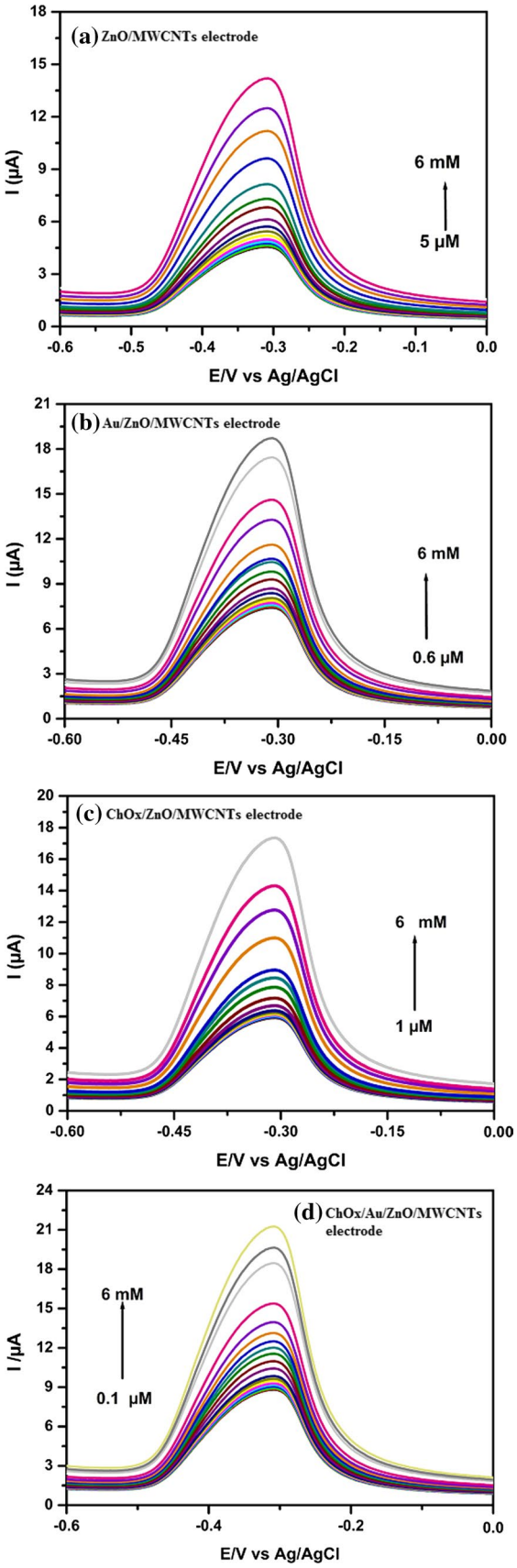

Fig. 7 Differential pulse voltammograms of **a** ZnO/MWCNTs, **b** ▶ Au/ZnO/MWCNTs, **c** ChOx/ZnO/MWCNTs and **d** ChOx/Au/ZnO/MWCNTs electrodes, examined at different cholesterol concentration ranging from 0.1 µM to 6 mM

Corresponding linear calibration curves (current versus cholesterol concentration) for all electrodes are depicted in Fig. 8. All electrodes show two linear ranges, less than 100 µM and from 100 µM to 6 mM of cholesterol concentration, respectively. Usually, the oxidation mechanism is adsorption for low concentration of cholesterol. But in high concentration of cholesterol the surface of electrode is occupied by cholesterol and there are insufficient available active sites for adsorption. So, two linear ranges can be detected in calibration curves. Limit of detection and sensitivity, extracted from DPV data based on first linear range of cholesterol concentration, is presented in Table 2. Comparing the results, the ChOx/Au/ZnO/MWCNTs electrode shows considerable low detection limit and high sensitivity.

To investigate the repeatability of ChOx/Au/ZnO/MWCNTs electrode, the experiment was repeated 10 times by one electrode in 10 µM cholesterol in PBS (pH 7.0) solution. The DPV results showed the relative standard deviation (RSD) value equal to 4.17%. The stability of ChOx/Au/ZnO/MWCNTs electrode was also studied by performing DPV in 10 µM cholesterol in PBS (pH 7.0) solution over 30 days. The DPV results demonstrated that the ChOx/Au/ZnO/MWCNTs electrode retains 96% of initial current response after 30 days, signifying that the electrode provides excellent stability on repeated detection of cholesterol.

Usually, the species like glucose, uric acid and many others are existed in biological liquid along with cholesterol. Therefore, it is highly likely these compounds interfere in the detection of cholesterol and it is crucial to study the anti-interference properties. The selectivity of ChOx/Au/ZnO/MWCNTs electrode toward cholesterol sensing was investigated in the presence of glucose and uric acid as interfering substances in the determination of 10 µM cholesterol in PBS (pH 7.0). The oxidation peak of cholesterol was observed around potential of − 0.32 V, while that of uric acid and glucose was detected around +0.38 V and +0.3 V, respectively. Table 3 displays interferences in successive addition of glucose and uric acid in the same cholesterol concentration. Results showed glucose and uric acid did not interfere in the determination of cholesterol up to 450-fold and 300-fold concentrations, respectively. Influence of glucose and uric acid as interfering substances in current density during cholesterol sensing is shown in Fig. 9. The amount of tolerance limit changes the current density for ± 5.0%.

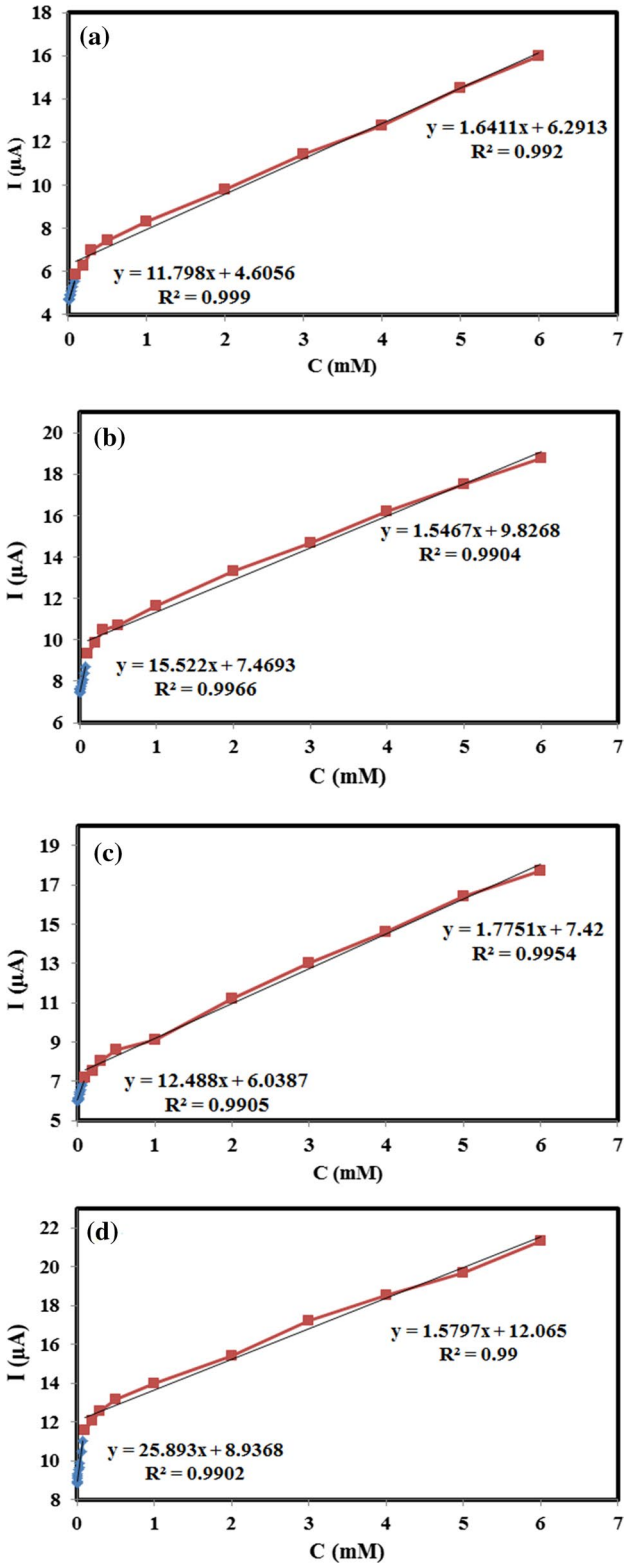

Fig. 8 Calibration graphs for **a** ZnO/MWCNTs, **b** Au/ZnO/MWCNTs, **c** ChOx/ZnO/MWCNTs and **d** ChOx/Au/ZnO/MWCNTs electrodes, extracted from DPV data

Table 2 Limit of detection and sensitivity of four fabricated electrodes, extracted from DPV data

Sensing electrode	LOD (μM)	Sensitivity (μA/μM)	Detection range(μM)
ZnO/MWCNTs	5	11.80	5–100
Au/ZnO/MWCNs	0.6	15.52	0.6–100
ChOx/ZnO/MWCNTs	1	12.49	1–100
ChOx/Au/ZnO/MWCNs	0.1	25.89	0.1–100

Table 3 The interference from glucose and uric acid on the voltammetric response in cholesterol sensing

Interfering substance	Concentration of interfering (Folds vs sample)	Relative standard deviation RSD (%)
Glucose	450	1
Uric acid	300	1.65

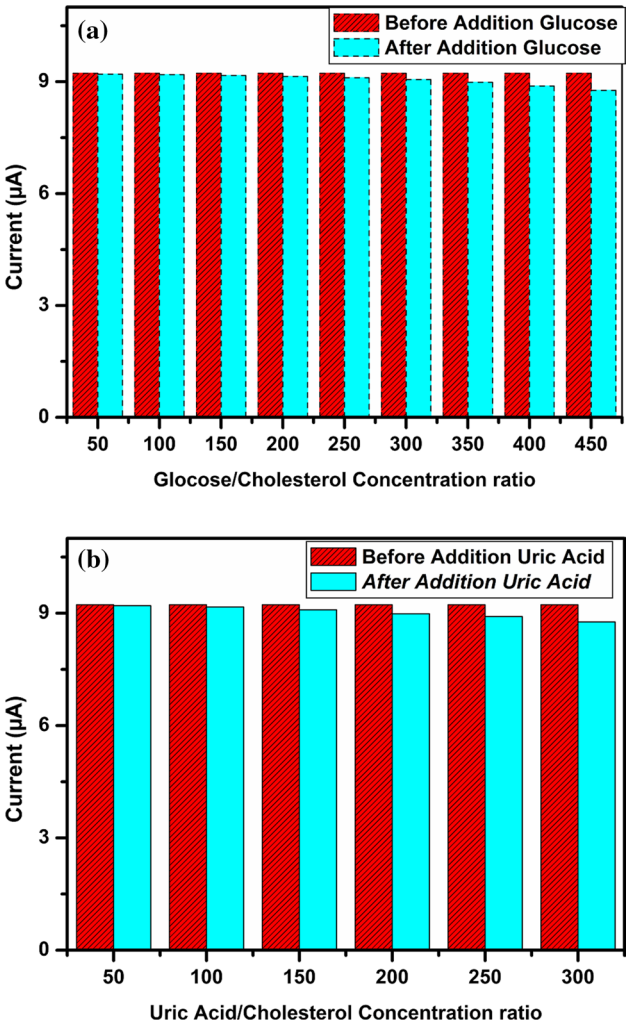

Fig. 9 Influence of **a** glucose and **b** uric acid as interfering substances on the DPV peak height of cholesterol (10 μM) in PBS (pH 7.0)

Table 4 Analysis of cholesterol content in human blood serum samples

Serum sample	Labeled concentration (mg/dL)	Labeled concentration (mM)	Determined cholesterol concentration (mM)
A	133	3.43	3.40
B	140	3.61	3.63
C	157	4.05	4.04
D	167	4.31	4.35

The reliability of the ChOx/Au/ZnO/MWCNTs electrode was also evaluated by the determination of cholesterol in human blood serum samples. The samples were obtained from healthy volunteers and the adequate amounts of serum samples were diluted with 30 mL PBS (pH 7.0). An oxidation peak of cholesterol was observed around the potential of − 0.32 V on the differential pulse voltammograms for all the real samples. DPV results and calibration curve were employed in the quantification of cholesterol content in these samples (Table 4). Equivalent value of what is expected and what mean value of five experiments shows, highlights the efficiency of ChOx/Au/ZnO/MWCNTs electrode in the quantitative determination of cholesterol in human blood serum. The recovery percentage was found to be > 99% with a minimum value of RSD.

In evaluation, the performance of the fabricated biosensor is compared with some of the previously reported cholesterol biosensors based on MWCNTs (Table 5). Considering the advantages, like good electrochemical behavior, high sensitivity, low detection limit, and easy fabrication, concluded that the presented electrode could be used as a good candidate for the detection of cholesterol, although further investigation can be done to optimize its performance. Furthermore, it has the potential for photoelectrochemical biosensing due to the unique and superior optical properties of ZnO and Au nanoparticles that could be investigated.

Conclusion

In this study, an enzymatic cholesterol biosensor was fabricated based on Au/ZnO/MWCNTs nanocomposite. Au/ZnO/MWCNTs nanocomposite was prepared by sol–gel method and deposited on FTO substrate by dip coating followed by ChOx stabilization. XRD results confirmed the formation of Au/ZnO/MWCNTs nanocomposites. FESEM images revealed that ZnO and Au nanoparticles decorated carbon nanotubes. FTIR results showed the functionalization of the nanotubes, as well as finger print peaks related to zinc oxide. The performances of the ChOx/Au/ZnO/MWCNTs electrode were characterized with CV, Nyquist plot (EIS) and DPV. The well-defined redox peaks indicated that the oxidation–reduction rate increased with increase in cholesterol concentration in a wide linear range. Also, conductivity and electron transfer rate on modified electrode increased due to high enzyme immobilization and direct electron transfer between the active sites of immobilized ChOx and FTO substrate by decoration of ZnO and Au nanoparticles on MWCNTs. A limit of detection of 0.1 µM and sensitivity of 25.89 µA/µM were obtained based on the first linear ranges of DPV calibration curve. The modified electrode also displayed good stability, repeatability and high selectivity toward cholesterol sensing in the presence of other interfering substances such as glucose and uric acid and was effectively applied to determine cholesterol in human blood serum samples.

Table 5 Performance comparison of the proposed cholesterol biosensor with the some previously reported ones

Sensing electrode	LOD (M)	Linearity Range (M)	Type of detection	References
MWCNT/ZnO	0.05 × 10−9	0.2 × 10−9–60.0 × 10−9	Cyclic voltammetry	[15]
ChOx/Au/MWCNT	0.02 × 10−3	0.18 × 10−3–11 × 10−3	Cyclic voltammetry	[8]
ChOx/MWCNTs	0.13 × 10−6	0.16 × 10−3–9.69 × 10−3	Amperometry	[7]
ChOx/Au/MWCNT	0.1 × 10−4	–	Amperometry	[27]
printed carbon electrode, MWCNTs, β-cyclodextrin	0.5 × 10−9	1 × 10−9–3 × 10−9	Differential Pulse Voltammetry	[28]
ChOx/ZnO/MWCNTs	1 × 10−6	1 × 10−6–100 × 10−6	Differential pulse voltammetry	This work
ChOx/Au/ZnO/MWCNs	0.1 × 10−6	0.1 × 10−6–100 × 10−6	Differential pulse voltammetry	This work

References

1. Baynes, J.W., Dominiczak, M.: Medical Biochemistry, 2nd edn. Elsevier, Amsterdam (2005)
2. Li, L.H., Dutkiewicz, E.P., Huang, Y.C., Zhou, H.B., Hsu, C.C.: Analytical methods for cholesterol quantification. J. Food Drug Anal. (2019). https://doi.org/10.1016/j.jfda.2018.09.001
3. Li, R., Xiong, C., Xiao, Z., Ling, L.: Colorimetric detection of cholesterol with G-quadruplex-based DNAzymes and ABTS2-. Anal. Chim. Acta (2012). https://doi.org/10.1016/j.aca.2012.02.015
4. Dervisevic, M., Çevik, E., Şenel, M., Nergiz, C., Abasiyanik, M.F.: Amperometric cholesterol biosensor based on reconstituted cholesterol oxidase on boronic acid functional conducting polymers. J. Electroanal. Chem. (2016). https://doi.org/10.1016/j.jelechem.2016.06.033
5. Molaei, R., Sabzi, R.E., Farhadi, K., Kheiri, F., Forough, M.: Amperometric biosensor for cholesterol based on novel nanocomposite array gold nanoparticles/acetone-extracted propolis/multiwall carbon nanotubes/gold. Micro Nano Lett. (2014). https://doi.org/10.1049/mnl.2013.0664
6. Saxena, U., BikasDas, A.: Nanomaterials towards fabrication of cholesterol biosensors: key roles and design approaches. Biosens. Bioelectron. (2016). https://doi.org/10.1016/j.bios.2015.08.042
7. Devi, S., Rodrigues, F., Meenakshi, S., Pandian, K., Perumal, P.: Carbon nanotube based amperometric biosensor for the quantitative detection of cholesterol. Biotechnol. Biochem. (2017). https://doi.org/10.9790/264X-03021020
8. Cai, X., Gao, X., Wang, L., Wu, Q., Lin, X.: A layer-by-layer assembled and carbon nanotubes/gold nanoparticles-based bienzyme biosensor for cholesterol detection. Chemi. Sens Actuators B (2013). https://doi.org/10.1016/j.snb.2013.02.050
9. Lin, X., Ni, Y., Kokot, S.: Electrochemical cholesterol sensor based on cholesterol oxidase and MoS_2-AuNPs modified glassy carbon electrode. Sens Actuators B: Chem. (2016). https://doi.org/10.1016/j.snb.2016.04.019
10. Mokwebo, K.V., Oluwafemi, O.S., Arotiba, O.A.: An electrochemical cholesterol biosensor based on a CdTe/CdSe/ZnSe quantum dots-poly (propylene imine) dendrimer nanocomposite immobilisation layer. Sensors (2018). https://doi.org/10.3390/s18103368
11. Ghosh, S., Ahmad, R., Khare, S.K.: Immobilization of cholesterol oxidase: an overview. Open Biotechnol. J. (2018). https://doi.org/10.2174/1874070701812010176
12. Zhu, Z.: An overview of carbon nanotubes and graphene for biosensing applications. Nano-Micro Lett. **9**, 1–24 (2017). https://doi.org/10.1007/s40820-017-0128-6
13. Sireesha, M., Jagadeesh Babu, V., Kranthi Kiran, A.S., Ramakrishna, S.: A review on carbon nanotubes in biosensor devices and their applications in medicine. Nanocomposites (2018). https://doi.org/10.1080/20550324.2018.1478765
14. Baldo, S., Buccheri, S., Ballo, A., Camarda, M., La Magna, A., Castagna, M.E., Romano, A., Iannazzo, D., Raimondo, F.D., Neri, G., Scalese, S.: Carbon nanotube-based sensing devices for human arginase-1 detection. Sens Bio-Sens. Res (2016). https://doi.org/10.1016/j.sbsr.2015.11.011
15. Gupta, V.K., Norouzi, P., Ganjali, H., Faridbod, F., Ganjali, M.R.: Flow injection analysis of cholesterol using FFT admittance voltammetric biosensor based on MWCNT–ZnO nanoparticles. Electrochim. Acta (2013). https://doi.org/10.1016/j.electacta.2013.03.118
16. Zhang, C., Wang, G., Ji, Y., Liu, M., Feng, Y., Zhang, Z., Fang, B.: Enhancement in analytical hydrazine based on gold nanoparticles deposited on ZnO-MWCNTs films. Sens Actuators B: Chem. (2010). https://doi.org/10.1016/j.snb.2010.07.007
17. Mehmood, S., Carlino, E., Bhatti, A.S.: Role of Au(NPs) in the enhanced response of Au(NPs)-decorated MWCNT electrochemical biosensor. Int. J. Nanomed. (2018). https://doi.org/10.2147/IJN.S155388
18. Gahlaut, A., Hooda, V., Dhull, V., Hooda, V.: Recent approaches to ameliorate selectivity and sensitivity of enzyme based cholesterol biosensors: a review. Artif. Cells Nanomed. Biotechnol. (2017). https://doi.org/10.1080/21691401.2017.1337028
19. Solanki, P.R., Kaushik, A., Ansari, A.A., Malhotra, B.D.: Nanostructured zinc oxide platform for cholesterol sensor. Appl. Phys. Lett. (2009). https://doi.org/10.1063/1.3111429
20. Zhao, Z., Lei, W., Zhang, X., Wang, B., Jiang, H.: ZnO-based amperometric enzyme biosensors. Sensors (Basel) (2010). https://doi.org/10.3390/s100201216
21. Paliwal, A., Gaur, R., Sharma, A., Tomar, M., Gupta, Vinay: Sensitive optical biosensor based on surface plasmon resonance using ZnO/Au bilayered structure. Optik (2016). https://doi.org/10.1016/j.ijleo.2016.05.103
22. Zang, Y., Fan, J., Yun, J., Xue, H., Pang, H.: Current advances in semiconductor nanomaterial-based photoelectrochemical biosensing. Eur. J. Chem. (2018). https://doi.org/10.1002/chem.201801358
23. Cullity, B.D., Stock, S.R.: Elements of X-ray diffraction, vol. 3. Prentice Hall, New-Jersey (2001)
24. Ahmed, D.S., Haider, A.J., Mohammad, M.R.: Comparesion of functionalization of multi walled carbon nanotubes treated by oil olive and nitric acid andtheircharacterization. Energy Procedia (2013). https://doi.org/10.1016/j.egypro.2013.07.126
25. Finnie, K.S., Cassidy, D.J., Bartlett, J.R., Woolfrey, J.L.: IR spectroscopy of surface water and hydroxyl species on nanocrystalline TiO_2 films. Langmuir (2001). https://doi.org/10.1021/la0009240
26. Vafaee, M., Ghamsari, M.S.: Preparation and characterization of ZnO nanoparticles by a novel sol–gel route. Mater. Lett. (2007). https://doi.org/10.1016/j.matlet.2006.11.089
27. Alagappan, M., Immanuel, S., Sivasubramanian, R., Kandaswamy, A.: Development of cholesterol biosensor using Au nanoparticles decorated f-MWCNT covered with polypyrrole network. Arab. J. Chem. (2018). https://doi.org/10.1016/j.arabjc.2018.02.018
28. Azhar, M., Nawaz, H., Majdinasab, M., Latif, U., Nasir, M., Gokce, G., WaqasAnwar, M., Hayat, A.: Development of a disposable electrochemical sensor for detection of cholesterol using differential pulse voltammetry. J. Pharm. Biomed. Anal. (2018). https://doi.org/10.1016/j.jpba.2018.07.005